

Dirac-Electron Behavior for Spin-Up Electrons in Strongly Interacting Graphene on Ferromagnetic Mn_5Ge_3

Elena Voloshina^{1,2,*} and Yuriy Dedkov^{1,†}

¹*Department of Physics, Shanghai University, 99 Shangda Road, 200444 Shanghai, China*

and

²*Physical and Theoretical Chemistry, Freie Universität Berlin, 14195 Berlin, Germany*

(Dated: June 4, 2019)

Abstract

An elegant approach on the synthesis of graphene on the strong ferromagnetic (FM) material Mn_5Ge_3 is proposed via intercalation of Mn in the graphene-Ge(111) interface. According to the DFT calculations, graphene in this strongly interacting system demonstrates the large exchange splitting of the graphene-derived π band. In this case only spin-up electrons in graphene preserve the Dirac-electron-like character in the vicinity of the Fermi level and the K point, whereas such behavior is not detected for the spin-down electrons. This unique feature of the studied gr/FM- Mn_5Ge_3 interface which can be prepared on the semiconducting Ge can lead to its application in spintronics.

This document is the unedited author's version of a Submitted Work that was subsequently accepted for publication in J. Phys. Chem. Lett., copyright © American Chemical Society after peer review. To access the final edited and published work see doi: 10.1021/acs.jpcclett.9b00893.

* Corresponding author. E-mail: voloshina@shu.edu.cn

† Corresponding author. E-mail: dedkov@shu.edu.cn

The recent progress in the intensive studies of the graphene-metal (gr-M) interfaces placed these systems in the forefront of the 2D-materials and particularly of the graphene-related research [1–3]. This situation is due to not only the perspectives of the mass-production of the high-quality graphene on metals [4, 5], but mainly because of the intriguing properties of the graphene-metal interface itself and that different gr-M systems are used as a playground in fundamental studies of the properties of 2D systems and as a basis for the preparation of more complex 2D-based heterosystems [6–8]. Among the gr-M systems the distinct attention is paid to the graphene-ferromagnet (gr-FM) interfaces and significant understanding of the properties of these systems has been achieved [9–11]. However, there are some factors which limit the further progress in the fundamental studies and in applications of these interesting objects. For example, the strong interaction at the gr-Ni(111) or gr-Co(0001) interfaces leads to the high degree of the $\pi - 3d$ hybridization of the valence band states at the interface between graphene and FM metal and, as a consequence, graphene loses its free-standing character and the carriers in the vicinity of the Fermi (E_F) level cannot be described as mass-less Dirac particles [9–12]. Yet, the same reason causes appearance of induced magnetic moments in graphene [13, 14]. In this case the states at E_F , which are significant for the description of the charge and spin transport properties of the junction, mainly have FM $3d$ character, substantially changing the band dispersion, states character and Fermi velocity of the carriers. Following works demonstrate the possibility to decouple graphene from the underlying FM material via intercalation of different species [2, 3], giving a route to restore the free-standing character of graphene, however losing the possibility of the induced spin polarization in a graphene layer [15–17].

Further progress in the graphene synthesis on different substrates and desire to implement graphene in the modern semiconductor technology led to the recent discovery of the graphene synthesis on the catalytically active semiconducting Ge substrates of different orientations [18]. This and subsequent studies demonstrate that Ge(110) and Ge(111) planes are more suitable for the graphene growth [19–21], whereas in case of Ge(001) a significant surface faceting under graphene layer [22, 23] was found limiting further technological processing of the later interface. The recent progress in this area is mainly focused on the studies of the growth mechanism of graphene on Ge surfaces and the studies of the electronic structure of gr-Ge interface or its modification are very rare [21, 23–25].

In the present work, we propose the elegant approach to prepare new gr-FM inter-

face, namely gr-Mn₅Ge₃, which combines several well approved steps used in the graphene-related studies. We performed density functional theory (DFT) calculations of the lattice-mismatched gr-Mn₅Ge₃(0001) interface in the super-cell geometry and it is computationally shown that in this strongly interacting system the graphene π states undergo strong exchange split leaving only spin-up electrons in the vicinity of E_F which preserve the Dirac-electron-like character for the carriers with the linear energy band dispersion. At the same time, for the spin-down electrons a series of localized interface states is formed that strongly reduces the carriers' mobility for this spin channel. Such difference for the electron mobilities **can** lead to the effective spin-filtering effect in such single-layer graphene-based junction. We believe that the described simple approach, which can be used for the preparation of this gr-FM interface, will be extremely useful in the future studies and applications, where 2D graphene as well as FM and semiconductor materials are included in one heterosystem. Details of DFT calculations and additional data are presented as the Supporting Information.

The preparation of the gr-Mn₅Ge₃(0001) interface can be accomplished in two steps (Figure 1). On the first step graphene is grown via chemical vapour deposition (CVD) or molecular beam epitaxy (MBE) on semiconducting Ge(111). As was demonstrated earlier [18], in this case graphene is aligned on this surface with the graphene zig-zag edges along the Ge $\langle 1\bar{1}0 \rangle$ and the arm-chair edges along Ge $\langle 11\bar{2} \rangle$. On the second preparation step a thin layer of FM metal Mn₅Ge₃(0001) can be grown under graphene via well established intercalation procedure, where thin Mn layer is deposited on graphene and then subsequently annealed at the elevated temperature. It is well known that FM Mn₅Ge₃(0001) can be epitaxially grown on Ge(111) in the temperature range 300 – 650° C [26–28] and it has relatively high Curie temperature of 296 K, which can be increased well above room temperature via chemical doping [29–32]. Also previous experiments demonstrate the gr/Ge interface is stable at temperatures, at least, up to 800° C [19, 21, 33]. Thus, the proposed preparation routine can lead to the epitaxial heterostructure consisting of 2D graphene, FM Mn₅Ge₃, and semiconducting Ge.

The crystallographic structure, top and side views, of the respective interfaces discussed above are shown in Figure 2. FM Mn₅Ge₃ has a hexagonal structure and it epitaxially grows on the Ge(111) surface forming the $(\sqrt{3} \times \sqrt{3})R30^\circ$ structure with respect to (1×1) -Ge(111) (Figure 2a). As described earlier, the gr-Mn₅Ge₃(0001) interface is formed via intercalation of a Mn layer in the gr-Ge(111) system. Two possible arrangements of C-atoms

on $\text{Mn}_5\text{Ge}_3(0001)$ are considered, structure B and structure T (FigureS1). Both structures are very similar with respect to their energetical stability (the difference in the interaction energy of graphene with substrate is of only 7 meV/C-atom). It is found that the discussed effects are valid for both structures and they are robust to the relative orientation of the layers at the gr- Mn_5Ge_3 interface. The resulting most energetically favourable interface (structure B) has the structure presented in Figure 2b, where the corresponding orientation of graphene with respect to the Ge(111) surface is preserved in order to avoid any layers rotations. For the formed gr- $\text{Mn}_5\text{Ge}_3(0001)$ interface the unit cell of the obtained structure has a periodicity of 5 unit cells of graphene and this unit cell (as well as the primitive unit cell of graphene) is rotated by 30° with respect to the unit cell of the underlying Mn_5Ge_3 . The side view of the fully relaxed gr- $\text{Mn}_5\text{Ge}_3(0001)$ interface is shown in Figure 2c with the mean distance between graphene and the top Mn layer of 2.144 Å. Considering the fact that the surface of Mn_5Ge_3 is Mn-terminated with the relatively small density of these atoms in the surface layer one can expect the appearance of the substantial corrugation of a graphene layer in this system. However, our calculations show that here graphene is quite flat with the corrugation of only 0.122 Å and the interaction energy of graphene with the $\text{Mn}_5\text{Ge}_3(0001)$ surface is 149.5 meV/C-atom, which places this system to the sub-class of a *strongly* interacting graphene with metallic substrate. The relatively small corrugation of graphene in the considered lattice mismatched system can be connected with the variation of the local environment for carbon atoms on the distance of not more than 2 carbon rings. The strong sp^2 character of carbon atoms in graphene and the rigidity of the σ bonds prevents the strong long-distance corrugation effect for the graphene layer. The flatness of graphene in this system might be crucial for the use of this interface as a spin filter thus avoiding the strong charge and spin scattering due to the interface corrugation on the atomic level. The simulated scanning tunnelling microscopy (STM) images of the $\text{Mn}_5\text{Ge}_3(0001)$ surface before and after graphene adsorption are shown in FigureS2 and can be used as a reference for the future experimental studies. The theoretical STM results for the clean surface are in very good agreement with the available experimental and theoretical data [26, 28, 34] confirming the correctness of the approach used in the present study.

Before adsorption of graphene on $\text{Mn}_5\text{Ge}_3(0001)$ the density of states of this material is strongly exchange split (Figure 3a and FigureS3). The magnetic moment of the surface Mn-(S) atoms is $3.48\mu_B$, which is larger compared to the value of $3.11\mu_B$ for the subsurface

Mn-(S-1) atoms, that can be explained by the reduced number of neighbours at the surface and the respective narrowing of the Mn $3d$ band. Adsorption of graphene leads to the substantial reduction of the magnetic moment of Mn-(S) and Mn-(S-1) to $3.11\mu_B$ and $2.98\mu_B$, respectively, which is reflected as the decrease of the exchange splitting of the respective states in Mn-atom projected partial DOS (PDOS) (Figure 3b). At the same time the π states of graphene become spin polarized due to the presence of the FM Mn_5Ge_3 substrate (Figure 3c). The calculated DOS for structure T and magnetic moments for all atoms in the studied systems can be found in Figure S4, in Table S5, and in the Supplementary data files.

The space-, energy, and k -vector overlap of the valence band states of graphene and Mn_5Ge_3 leads to the effective hybridization of these states. At the same time the spin character of these states is also conserved in this process. This can be clearly seen in Figure S6 where large-energy scale band structures of the gr/ $\text{Mn}_5\text{Ge}_3(0001)$ interface obtained after unfolding procedure are shown (for comparison reasons, in case of structure B, DFT calculations were performed with and without inclusion of the spin-orbit interaction). Considering the DOS of Mn_5Ge_3 (Figure 3a,b and shadowed areas in Figure S6) we can clearly see that spin-polarized graphene π bands hybridize with the Mn-atoms projected valence band states of the only respective spin character. This effect leads to the “huge” band gaps for both graphene π bands of different spin characters around the K point of the graphene-derived (1×1) Brillouin zone: for spin-up states this gap is between $E - E_F \approx -3.8\text{eV} \dots - 0.5\text{eV}$ and for spin-down states this gap is between $E - E_F \approx -1.4\text{eV} \dots + 2.1\text{eV}$. At the same time the effect of hybridization leads to the appearance of the so-called interface states of the mixed graphene- π and Mn $3d$ character, which manifest themselves as a series of flat bands of the respective spin character in the energy range $E - E_F \approx -3.8\text{eV} \dots + 2.1\text{eV}$. The similar effect of the interface states formation was observed earlier for other gr-FM interfaces, gr/Ni(111) and gr/Co(0001) [9, 10, 15, 35, 36].

The effect of the spin-conservation during hybridization of the valence band states at the gr- $\text{Mn}_5\text{Ge}_3(0001)$ interface leads to the interesting results, which have dramatic implications on the spin-filtering properties of this interface. Analysis of the zoomed region around the K point and in the vicinity of E_F of the band structure of this system showed in Figure 3d,e demonstrates that only spin-up electrons in graphene retain the Dirac-electron-like character with the linear energy dispersion for these electronic states. There is a clear

anisotropy for the band dispersion along the $\Gamma - K$ and $M - K$ directions and the linear fit of the graphene π band around E_F gives the Fermi velocity of $v_F = 0.(92 \pm 0.01) \times 10^6 \text{m/s}$ and $v_F = 0.(71 \pm 0.01) \times 10^6 \text{m/s}$ for $\Gamma - K$ and $M - K$, respectively, which is very close to the value characteristic for free-standing graphene and which is much higher compared to the value which was extracted for the strongly hybridized states formed at the gr/Co(0001) interface [11]. Moreover, this spin-up state has a linear dispersion in the energy range of $\approx 1\text{eV}$ around E_F that significantly simplifies the energy position control for this state. For spin-down electrons, there is a relatively large gap between $E - E_F \approx -1.2\text{eV} \dots +0.1\text{eV}$ at the K point. Above and below this energy window a series of the interface states is formed which was described above. The carriers on these states have very small group velocity due to the relatively large Mn $3d$ character. All these factors allow us to conclude that the contact of graphene with FM- Mn_5Ge_3 will have a strong influence on its spin-transport properties.

In conclusion, we have discovered a new interface of graphene with strong ferromagnetic material Mn_5Ge_3 , which valence band states are strongly exchange split. This system can be easily fabricated using two steps preparation routine: CVD or MBE of graphene on the catalytically active Ge(111) surface and then intercalation of Mn in the gr-Ge(111) interface with the formation of the ordered gr- $\text{Mn}_5\text{Ge}_3(0001)$ interface. Our systematic large-scale DFT calculations for this interface demonstrate that graphene is relatively strongly bonded to the FM Mn_5Ge_3 substrate that leads to the substantial exchange splitting of the graphene π states. It is found that the effect of the spin-conservation during hybridization of the graphene π and Mn $3d$ valence band states leads to the appearance of the large band gaps in the energy dispersion of the graphene π states for both spin channels. The unique combination of all factors leads to the observation of the only spin-up electrons of graphene at the K point and at E_F which conserve the Dirac-electron-like character. At the same time for the spin-down electrons the band gap is found at E_F . We expect that our study will stimulate future experimental effort to create graphene-semiconductor and graphene-FM structures and we can expect that the possible 2D graphene - FM Mn_5Ge_3 - semiconducting Ge systems will be used in the charge and spin transport studies and applications.

The North-German Supercomputing Alliance (HLRN) is acknowledged for providing com-

puter time.

-
- [1] Geim, A. Graphene: Status and Prospects. *Science* **2009**, *324*, 1530–1534.
- [2] Batzill, M. The surface science of graphene: Metal interfaces, CVD synthesis, nanoribbons, chemical modifications, and defects. *Surf. Sci. Rep.* **2012**, *67*, 83–115.
- [3] Dedkov, Y.; Voloshina, E. Graphene growth and properties on metal substrates. *J. Phys.: Condens. Matter* **2015**, *27*, 303002.
- [4] Bae, S.; Kim, H.; Lee, Y.; Xu, X.; Park, J.-S.; Zheng, Y.; Balakrishnan, J.; Lei, T.; Kim, H. R.; Song, Y. I. et al. Roll-to-roll production of 30-inch graphene films for transparent electrodes. *Nat. Nanotech.* **2010**, *5*, 574–578.
- [5] Ryu, J.; Kim, Y.; Won, D.; Kim, N.; Park, J. S.; Lee, E.-K.; Cho, D.; Cho, S.-P.; Kim, S. J.; Ryu, G. H. et al. Fast Synthesis of High-Performance Graphene Films by Hydrogen-Free Rapid Thermal Chemical Vapor Deposition. *ACS Nano* **2014**, *8*, 950–956.
- [6] Meng, L.; Wu, R.; Zhou, H.; Li, G.; Zhang, Y.; Li, L.; Wang, Y.; Gao, H.-J. Silicon intercalation at the interface of graphene and Ir(111). *Appl. Phys. Lett.* **2012**, *100*, 083101.
- [7] Xie, C.; Jiang, S.; Zou, X.; Sun, Y.; Zhao, L.; Hong, M.; Chen, S.; Huan, Y.; Shi, J.; Zhou, X. et al. Space-confined growth of monolayer ReSe₂ under a graphene layer on Au foils. *Nano Res.* **2018**, *12*, 149–157.
- [8] Ehlen, N.; Hall, J.; Senkovskiy, B. V.; Hell, M.; Li, J.; Herman, A.; Smirnov, D.; Fedorov, A.; Yu Voroshnin, V.; Di Santo, G. et al. Narrow photoluminescence and Raman peaks of epitaxial MoS₂ on graphene/Ir(111). *2D Materials* **2019**, *6*, 011006–21.
- [9] Dedkov, Y. S.; Fonin, M. Electronic and magnetic properties of the graphene–ferromagnet interface. *New J. Phys.* **2010**, *12*, 125004.
- [10] Voloshina, E.; Dedkov, Y. In *Physics and Applications of Graphene - Experiments*; Mikhailov, S., Ed.; InTech: Rijeka, 2011; pp 329–352.
- [11] Usachov, D.; Fedorov, A.; Otrokov, M. M.; Chikina, A.; Vilkov, O.; Petukhov, A.; Rybkin, A. G.; Koroteev, Y. M.; Chulkov, E. V.; Adamchuk, V. K. et al. Observation of Single-Spin Dirac Fermions at the Graphene/Ferromagnet Interface. *Nano Lett.* **2015**, *15*, 2396–2401.
- [12] Karpan, V. M.; Giovannetti, G.; Khomyakov, P. A.; Talanana, M.; Starikov, A. A.; Zwierzycki, M.; Brink, J. v. d.; Brocks, G.; Kelly, P. J. Graphite and Graphene as Perfect Spin Filters.

Phys. Rev. Lett. **2007**, *99*, 176602.

- [13] Weser, M.; Rehder, Y.; Horn, K.; Sicot, M.; Fonin, M.; Preobrajenski, A. B.; Voloshina, E. N.; Goering, E.; Dedkov, Y. S. Induced magnetism of carbon atoms at the graphene/Ni(111) interface. *Appl. Phys. Lett.* **2010**, *96*, 012504.
- [14] Matsumoto, Y.; Entani, S.; Koide, A.; Ohtomo, M.; Avramov, P. V.; Naramoto, H.; Amemiya, K.; Fujikawa, T.; Sakai, S. Spin orientation transition across the single-layer graphene/nickel thin film interface. *J. Mater. Chem. C* **2013**, *1*, 5533.
- [15] Voloshina, E. N.; Generalov, A.; Weser, M.; Böttcher, S.; Horn, K.; Dedkov, Y. S. Structural and electronic properties of the graphene/Al/Ni(111) intercalation system. *New J. Phys.* **2011**, *13*, 113028.
- [16] Vita, H.; Böttcher, S.; Horn, K.; Voloshina, E. N.; Ovcharenko, R. E.; Kampen, T.; Thissen, A.; Dedkov, Y. S. Understanding the origin of band gap formation in graphene on metals: graphene on Cu/Ir(111). *Sci. Rep.* **2014**, *4*, 5704.
- [17] Omiciuolo, L.; ndez, E. R. H. a.; Miniussi, E.; Orlando, F.; Lacovig, P.; Lizzit, S.; scedil, T. O. M.; Locatelli, A.; Larciprete, R.; Bianchi, M. et al. Bottom-up approach for the low-cost synthesis of graphene-alumina nanosheet interfaces using bimetallic alloys. *Nat. Commun.* **2014**, *5*, 5062.
- [18] Lee, J.-H.; Lee, E. K.; Joo, W.-J.; Jang, Y.; Kim, B.-S.; Lim, J. Y.; Choi, S.-H.; Ahn, S. J.; Ahn, J. R.; Park, M.-H. et al. Wafer-scale growth of single-crystal monolayer graphene on reusable hydrogen-terminated germanium. *Science* **2014**, *344*, 286–289.
- [19] Kiraly, B.; Jacobberger, R. M.; Mannix, A. J.; Campbell, G. P.; Bedzyk, M. J.; Arnold, M. S.; Hersam, M. C.; Guisinger, N. P. Electronic and Mechanical Properties of Graphene–Germanium Interfaces Grown by Chemical Vapor Deposition. *Nano Lett.* **2015**, *15*, 7414–7420.
- [20] Wang, H.; Yu, G. Direct CVD Graphene Growth on Semiconductors and Dielectrics for Transfer-Free Device Fabrication. *Adv. Mater.* **2016**, *28*, 4956–4975.
- [21] Tesch, J.; Paschke, F.; Fonin, M.; Wietstruk, M.; Böttcher, S.; Koch, R. J.; Bostwick, A.; Jozwiak, C.; Rotenberg, E.; Makarova, A. et al. The graphene/n-Ge(110) interface: structure, doping, and electronic properties. *Nanoscale* **2018**, *10*, 6088–6098.
- [22] Pasternak, I.; Dabrowski, P.; Ciepielewski, P.; Kolkovsky, V.; Klusek, Z.; Baranowski, J. M.; Strupiński, W. Large-area high-quality graphene on Ge(001)/Si(001) substrates. *Nanoscale* **2016**, *8*, 11241–11247.

- [23] Dabrowski, P.; Rogala, M.; Pasternak, I.; Baranowski, J.; Strupinski, W.; Kopciuszynski, M.; Zdyb, R.; Jalochoowski, M.; Lutsyk, I.; Klusek, Z. The study of the interactions between graphene and Ge(001)/Si(001). *Nano Res.* **2017**, *3*, 11700–14.
- [24] Zhou, D.; Niu, Z.; Niu, T. Surface Reconstruction of Germanium: Hydrogen Intercalation and Graphene Protection. *The Journal of Physical Chemistry C* **2018**, *122*, 21874–21882.
- [25] Ahn, S. J.; Kim, H. W.; Khadka, I. B.; Rai, K. B.; Ahn, J. R.; Lee, J.-H.; Kang, S. G.; Whang, D. Electronic Structure of Graphene Grown on a Hydrogen-terminated Ge (110) Wafer. *J. Korean Phys. Soc.* **2018**, *73*, 656–660.
- [26] Zeng, C.; Erwin, S. C.; Feldman, L. C.; Li, A. P.; Jin, R.; Song, Y.; Thompson, J. R.; Weitering, H. H. Epitaxial ferromagnetic Mn₅Ge₃ on Ge(111). *Appl. Phys. Lett.* **2003**, *83*, 5002–5004.
- [27] Dedkov, Y. S.; Holder, M.; Mayer, G.; Fonin, M.; Preobrajenski, A. B. Spin-resolved photoemission of a ferromagnetic Mn₅Ge₃(0001) epilayer on Ge(111). *J. Appl. Phys.* **2009**, *105*, 073909.
- [28] Grytzelius, J. H.; Zhang, H.; Johansson, L. S. Surface atomic and electronic structure of Mn₅Ge₃ on Ge(111). *Phys. Rev. B* **2011**, *84*.
- [29] Gajdzik, M.; Sürgers, C.; Kelemen, M. T.; Löhneysen, H. v. Strongly enhanced Curie temperature in carbon-doped Mn₅Ge₃ films. *Journal of Magnetism and Magnetic Materials* **2000**, *221*, 248–254.
- [30] Slipukhina, I.; Arras, E.; Mavropoulos, P.; Pochet, P. Simulation of the enhanced Curie temperature in Mn₅Ge₃C_x compounds. *Appl. Phys. Lett.* **2009**, *94*, 192505.
- [31] Stojilovic, N.; Dordevic, S. V.; Hu, R.; Petrovic, C. Effect of carbon doping on electronic transitions in Mn₅Ge₃. *J. Appl. Phys.* **2013**, *114*, 053708–6.
- [32] Petit, M.; Michez, L.; Dutoit, C.-E.; Bertaina, S.; Dolocan, V. O.; Heresanu, V.; Stoffel, M.; Le Thanh, V. Very low-temperature epitaxial growth of Mn₅Ge₃ and Mn₅Ge₃C_{0.2} films on Ge(111) using molecular beam epitaxy. *Thin Solid Films* **2015**, *589*, 427–432.
- [33] Tesch, J.; Voloshina, E.; Fonin, M.; Dedkov, Y. Growth and electronic structure of graphene on semiconducting Ge(110). *Carbon* **2017**, *122*, 428–433.
- [34] Zhang, H. M.; Grytzelius, J. H.; Johansson, L. S. O. Thin Mn germanide films studied by XPS, STM, and XMCD. *Phys. Rev. B* **2013**, *88*, 045311.
- [35] Bertoni, G.; Calmels, L.; Altibelli, A.; Serin, V. First-principles calculation of the electronic

- structure and EELS spectra at the graphene/Ni(111) interface. *Phys. Rev. B* **2004**, *71*, 075402.
- [36] Karpan, V. M.; Khomyakov, P. A.; Starikov, A. A.; Giovannetti, G.; Zwierzycki, M.; Talanana, M.; Brocks, G.; Brink, J. v. d.; Kelly, P. J. Theoretical prediction of perfect spin filtering at interfaces between close-packed surfaces of Ni or Co and graphite or graphene. *Phys. Rev. B* **2008**, *78*, 195419.

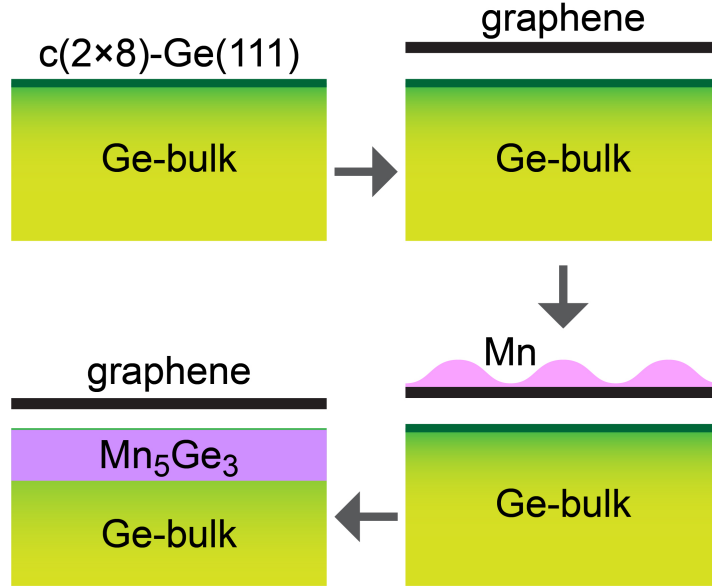


FIG. 1: Two-steps preparation procedure for the gr-Mn₅Ge₃(0001) system: (i) graphene on Ge(111) is grown via CVD or MBE; (ii) atomically sharp gr-Mn₅Ge₃(0001) interface is formed via intercalation of the pre-deposited thin layer of Mn on gr-Ge(111).

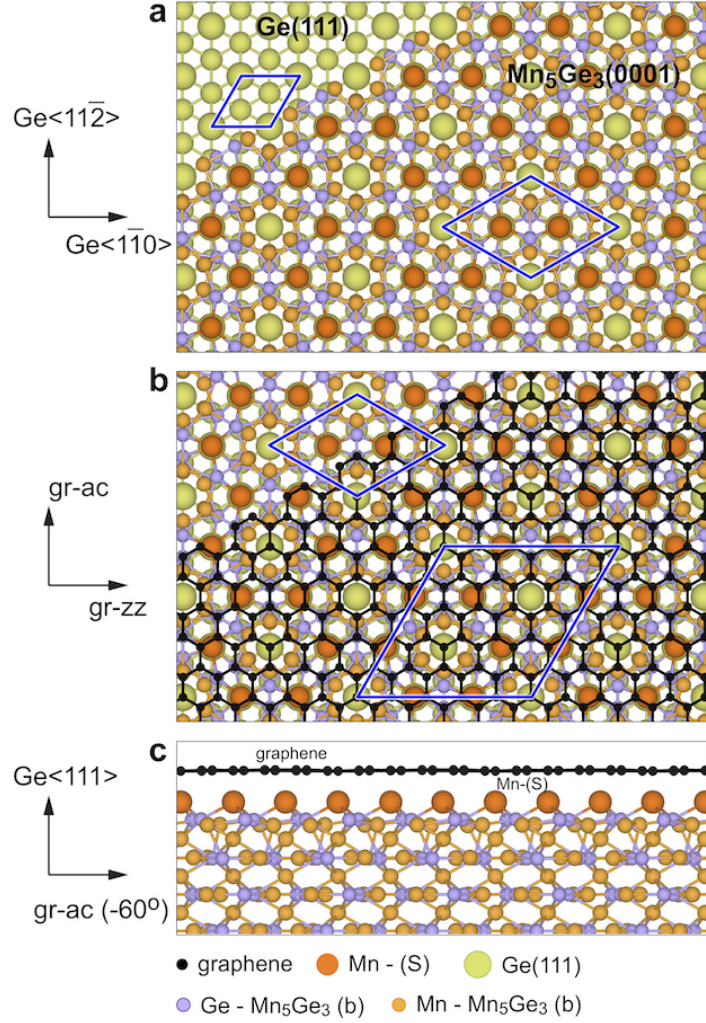


FIG. 2: Top views of the crystallographic structure of (a) Mn₅Ge₃(0001)/Ge(111) and (b) gr/Mn₅Ge₃(0001)/Ge(111) (structure B). (c) Side view of the fully relaxed optimized gr-Mn₅Ge₃(0001) interface (structure B). Blue rhombuses mark unit cells of (1 × 1)-Ge(111), (√3 × √3)R30°-Mn₅Ge₃(0001), and (5 × 5)-gr/Mn₅Ge₃(0001), respectively. Crystallographic directions of Ge-bulk as well as graphene arm-chair (ac) and zig-zag (zz) edges are marked on the left hand side of the image. Side view in (c) is taken for the view direction perpendicular to the main diagonal of the big rhombus in (b). Corresponding colored circles are used for carbon atoms in graphene and for Mn and Ge atoms in bulk (b) and at the interface (S).

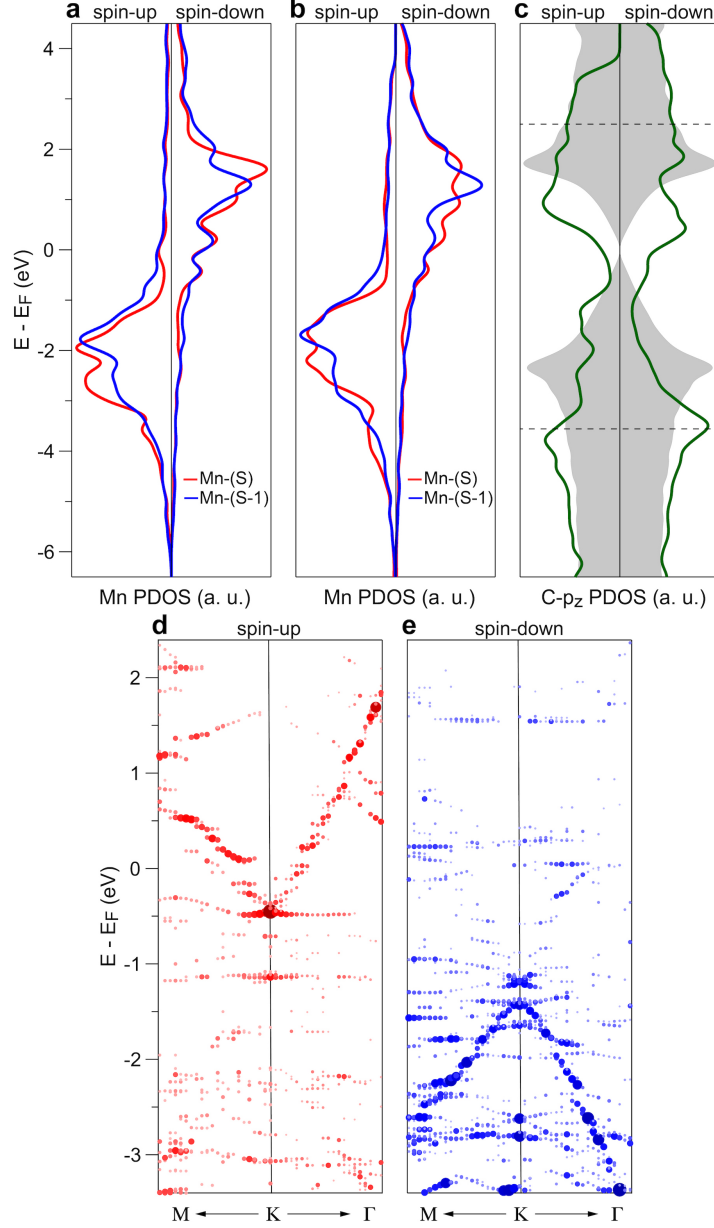


FIG. 3: Spin-resolved Mn-atom projected PDOS for (a) the clean Mn₅Ge₃(0001) surface and (b) the gr-Mn₅Ge₃(0001) interface (structure B). (c) Spin-resolved C-atom projected p_z PDOS for (5 × 5)-gr/Mn₅Ge₃(0001) (structure B). Grey shadowed area in (c) shows the C p_z PDOS for the free-standing graphene in the same (5 × 5) unit cell. (d,e) Spin-resolved band structure obtained after unfolding procedure and presented around the K point of the (1 × 1) graphene-derived Brillouin zone for the (5 × 5)-gr/Mn₅Ge₃(0001) system (structure B) for spin-up and spin-down channels, respectively. The size of the point gives the information about the number of primitive cell bands crossing particular (k, E) in the unfolded procedure, i. e. the partial density of states at (k, E) . Energy range in (d,e) corresponds to the one marked by the dashed lines in (c).

Supporting Information for: “Dirac-Electron Behavior for the Spin-Up Electrons in the Strongly Interacting Graphene on Ferromagnetic Mn₅Ge₃”

Computational Details

Spin-polarised DFT calculations based on plane-wave basis sets of 500 eV cutoff energy were performed with the Vienna *ab initio* simulation package (VASP) [1, 2]. The Perdew-Burke-Ernzerhof (PBE) exchange-correlation functional [3] was employed. The electron-ion interaction was described within the projector augmented wave (PAW) method [4] with C (*2s,2p*), Ge (*4s,4p*), and Mn (*3d,4s*) states treated as valence states. The Brillouin-zone integration was performed on Γ -centred symmetry reduced Monkhorst-Pack meshes using a Methfessel-Paxton smearing method of first order with $\sigma = 0.15$ eV, except for the calculations of total energies. For these calculations, the tetrahedron method with Blöchl corrections [5] was employed. The k mesh for sampling the supercell Brillouin zone are chosen to be as dense as $18 \times 18 \times 24$, $18 \times 18 \times 1$ and $12 \times 12 \times 1$ in the case of Mn₅Ge₃ bulk, Mn₅Ge₃ (0001) surface and gr/Mn₅Ge₃(0001) interface, respectively. Dispersion interactions were considered by adding a $1/r^6$ atom-atom term as parameterised by Grimme (“D2” parameterisation) [6]. For comparisons reasons, some calculations (results are marked in the respective figures) were performed with spin-orbit interaction taken into account. The calculated band structures were unfolded (where necessary) to the graphene (1×1) primitive unit cells according to the procedure described in Refs. 7, 8 with the code BandUP.

Bulk Mn₅Ge₃ is a ferromagnetic intermetallic compound. It crystallises in the hexagonal D_{8h} structure (prototype Mn₅Si₃ and space group $P6_3/mcm$) and has lattice parameters of $a = 7.184$ Å and $c = 5.053$ Å [9]. The hexagonal cell contains 10 Mn (two sub-lattices, Mn1 and Mn2) and 6 Ge atoms. Four atomic planes are situated perpendicular to the axis z . Planes $z = 0$ and $z = 1/2$ contain only Mn1-atoms, planes $z = 1/4$ and $z = 3/4$ contain Ge- and Mn2-atoms. Mn1-atoms are surrounded by 6 Ge-atoms and Mn2-atoms are surrounded by 5 Ge-atoms. The atomic positions are: Mn1 in 4(d) site: $\pm(1/3, 2/3, 0; 2/3, 1/3, 1/2)$; Mn2 in 6(g) site: $\pm(x_1, 0, 1/4; 0, x_1, 1/4; -x_1, -x_1, 1/4)$ with $x_1 = 0.2397$, Ge in 6(g) site: $\pm(x_2, 0, 1/4; 0, x_2, 1/4; -x_2, -x_2, 1/4)$ with $x_2 = 0.6030$. The optimised lattice parameters ($a = 7.145$ Å, $c = 4.976$ Å, $x_1 = 0.2435$, $x_2 = 0.6059$) were used in order to construct models for the (0001) surface as well as interface with graphene.

The $\text{Mn}_5\text{Ge}_3(0001)$ surface was modelled by a slab containing 12 atomic layers and a vacuum gap of approximately 23 \AA . The atoms of the 8 bottom layers were fixed at their bulk positions during the structural optimisation procedure, whereas the positions (x, y, z -coordinates) of all other atoms were fully relaxed until forces became smaller than 0.02 eV \AA^{-1} .

To model the $\text{gr}/\text{Mn}_5\text{Ge}_3(0001)$ interface, a $(\sqrt{3} \times \sqrt{3}) R30^\circ$ structure was formed with respect to $\text{Mn}_5\text{Ge}_3(0001)$ slab and its top side was covered by a graphene layer consisting of (5×5) unit cells. Thus, the resulting supercell has the size $(12.375 \text{ \AA} \times 12.375 \text{ \AA})$ and consists of 50 C-atoms, 90 Mn-atoms and 54 Ge-atoms. In the resulting structure the graphene lattice was stretched by 0.6% compared to the equilibrium lattice constant of 2.461 \AA . Two possible arrangements of C-atoms above the $\text{Mn}_5\text{Ge}_3(0001)$ surface were considered - structure B and structure T. In structure B (which is energetically more favourable one) all Mn atoms of the interface layer are bridged by the C-atoms of the graphene layer. Structure T is obtained by shift of a graphene layer in the (x, y) plane in such a way, that C atoms of graphene occupy all possible high-symmetry adsorption positions with respect to the interface Mn-layer. As for the clean surface, the atoms of the 8 bottom layers were fixed at their bulk positions during the structural optimization procedure, whereas the positions (x, y, z -coordinates) of all other atoms were fully relaxed until forces became smaller than 0.02 eV \AA^{-1} .

-
- [1] Kresse, G.; Hafner, J. *J. Phys.: Condens. Matter* **1994**, *6*, 8245–8257.
 - [2] Kresse, G.; Furthmuller, J. *Phys. Rev. B* **1996**, *54*, 11169–11186.
 - [3] Perdew, J.; Burke, K.; Ernzerhof, M. *Phys. Rev. Lett.* **1996**, *77*, 3865–3868.
 - [4] Blöchl, P. E. *Phys. Rev. B* **1994**, *50*, 17953–17979.
 - [5] Blöchl, P. E.; Jepsen, O.; Andersen, O. *Phys. Rev. B* **1994**, *49*, 16223–16233.
 - [6] Grimme, S. *J. Comput. Chem.* **2006**, *27*, 1787–1799.
 - [7] Medeiros, P. V. C.; Stafström, S.; Björk, J. *Phys. Rev. B* **2014**, *89*, 041407.
 - [8] Medeiros, P. V. C.; Tsirkin, S. S.; Stafström, S.; Björk, J. *Phys. Rev. B* **2015**, *91*, 041116.
 - [9] Forsyth, J. B.; Brown, P. J. *J. Phys.: Condens. Matter* **1999**, *2*, 2713.

List of Tables and Figures

Fig.S1: Top and side views of (a) structure B and (b) structure T. Corresponding colored circles are used for carbon atoms in graphene and for Mn and Ge atoms in bulk (b) and at the interface (S).

Fig.S2: Calculated STM images for (a) the clean $\text{Mn}_5\text{Ge}_3(0001)$ surface and for the gr/ $\text{Mn}_5\text{Ge}_3(0001)$ system – (b) structure B and (c) structure T. Bias voltages are marked in every image.

Fig.S3: Spin resolved band structures of (a) bulk Mn_5Ge_3 and (b) $\text{Mn}_5\text{Ge}_3(0001)$ surface. The respective Brillouin zones are shown on the right-hand side for every panel.

Fig.S4: Spin-resolved Mn-atom projected PDOS for (a) the clean $\text{Mn}_5\text{Ge}_3(0001)$ surface and (b) the gr/ $\text{Mn}_5\text{Ge}_3(0001)$ interface (structure T). (c) C-atom projected p_z PDOS for (5×5) -gr/ $\text{Mn}_5\text{Ge}_3(0001)$ (structure T). Grey shadowed area in (c) show the C p_z PDOS for the free-standing graphene in the same (5×5) unit cell.

Tab.S5: Parameters, interaction energy, distances between layers, and magnetic moments, for the $\text{Mn}_5\text{Ge}_3(0001)$ surface and gr/ $\text{Mn}_5\text{Ge}_3(0001)$ (structures B and T). All distances are marked according to Fig. S1. The respective structures can be visualized using software VESTA (<http://jp-minerals.org/vesta/en/>); instructions are placed as a header in every txt-file. Structures files are available upon request.

Fig.S6: Large-energy scale spin-resolved band structures for the gr/ $\text{Mn}_5\text{Ge}_3(0001)$ system shown for structure B without (a) and with (b) inclusion of the spin-orbit interaction. In (c) the large-energy scale spin-resolved band structure (without inclusion of the spin-orbit interaction) for structure T is shown. Data in (b) and (c) are shown only for $\Gamma - \text{K}$ direction. In (a), the discussed in the main text band gaps for the graphene π states are marked with E_g for spin-up and spin-down channels..

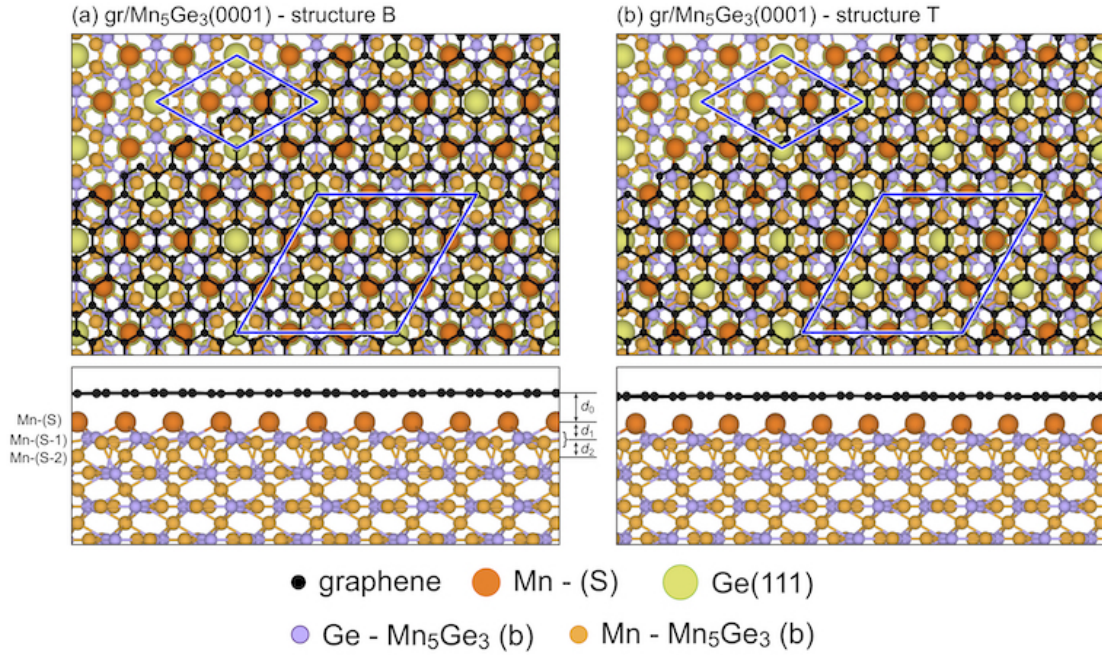


Fig. S1: Top and side views of (a) structure B and (b) structure T. Corresponding colored circles are used for carbon atoms in graphene and for Mn and Ge atoms in bulk (b) and at the interface (S).

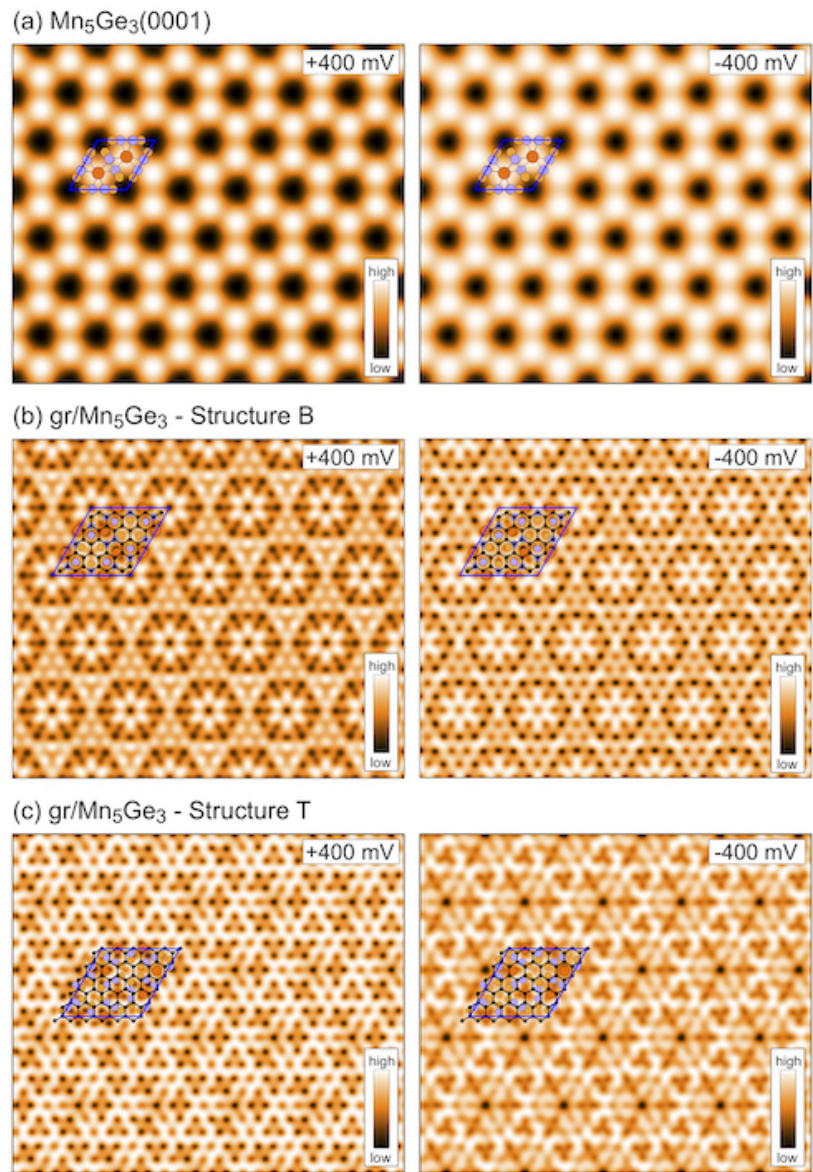


Fig. S2: Calculated STM images for (a) the clean $\text{Mn}_5\text{Ge}_3(0001)$ surface and for the gr/ $\text{Mn}_5\text{Ge}_3(0001)$ system – (b) structure B and (c) structure T. Bias voltages are marked in every image.

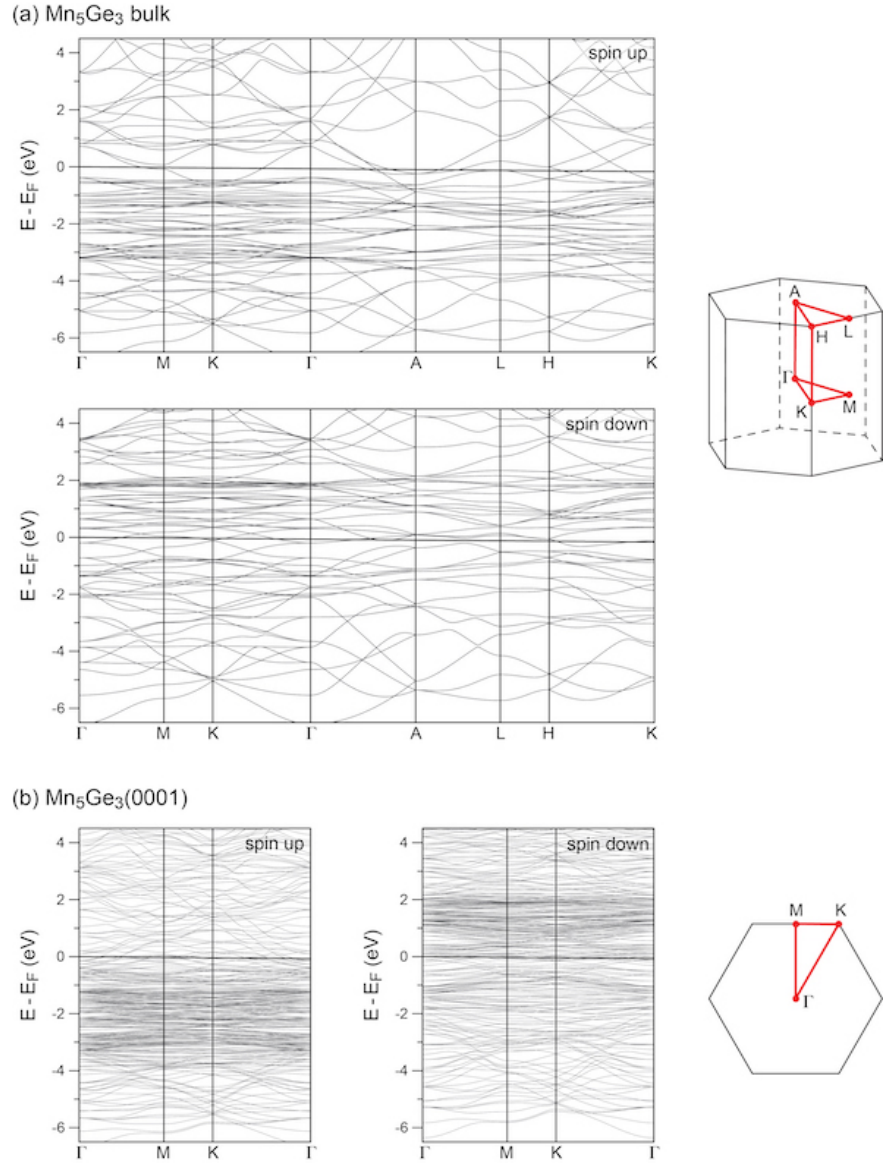


Fig. S3: Spin resolved band structures of (a) bulk Mn_5Ge_3 and (b) $\text{Mn}_5\text{Ge}_3(0001)$ surface. The respective Brillouin zones are shown on the right-hand side for every panel.

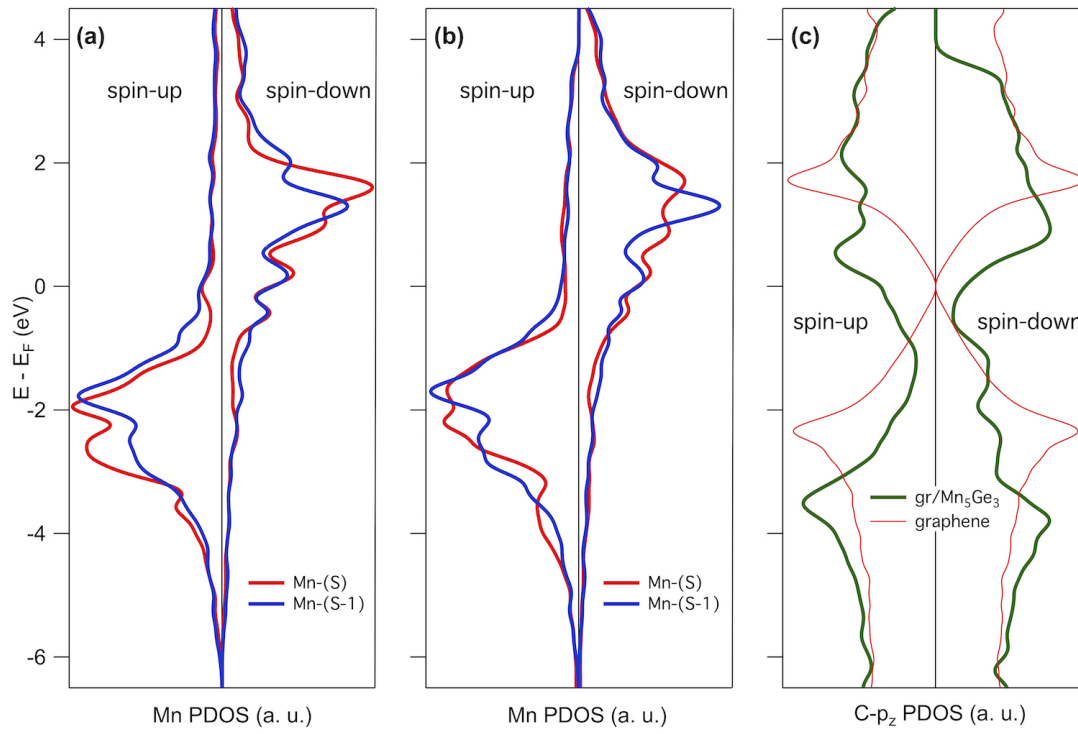


Fig. S4: Spin-resolved Mn-atom projected PDOS for (a) the clean $Mn_5Ge_3(0001)$ surface and (b) the $gr/Mn_5Ge_3(0001)$ interface (structure T). (c) C-atom projected p_z PDOS for (5×5) - $gr/Mn_5Ge_3(0001)$ (structure T). Thin line in (c) shows the C p_z PDOS for the free-standing graphene in the same (5×5) unit cell.

Table S5: Parameters, interaction energy, distances between layers, and magnetic moments, for the $\text{Mn}_5\text{Ge}_3(0001)$ surface and $\text{gr}/\text{Mn}_5\text{Ge}_3(0001)$ (structures B and T). All distances are marked according to Fig. S1. The respective structures can be visualized using software VESTA (<http://jp-minerals.org/vesta/en/>); instructions are placed as a header in every txt-file. Structures files are available upon request.

	$\text{Mn}_5\text{Ge}_3(0001)$	$\text{gr}/\text{Mn}_5\text{Ge}_3$	
		Structure B	Structure T
$E_{\text{int}}/\text{meV}$		-149.5	-142.6
$d_0/\text{\AA}$		2.144	2.137
$d_1/\text{\AA}$	1.286	1.377	1.378
$d_2/\text{\AA}$	1.232	1.144	1.145
$m_{\text{Mn(S)}}/\mu_B$	see Structure-surf.txt	see Structure-B.txt	see Structure-T.txt
$m_{\text{Mn(S-1)}}/\mu_B$	see Structure-surf.txt	see Structure-B.txt	see Structure-T.txt
m_{C}/μ_B	see Structure-surf.txt	see Structure-B.txt	see Structure-T.txt

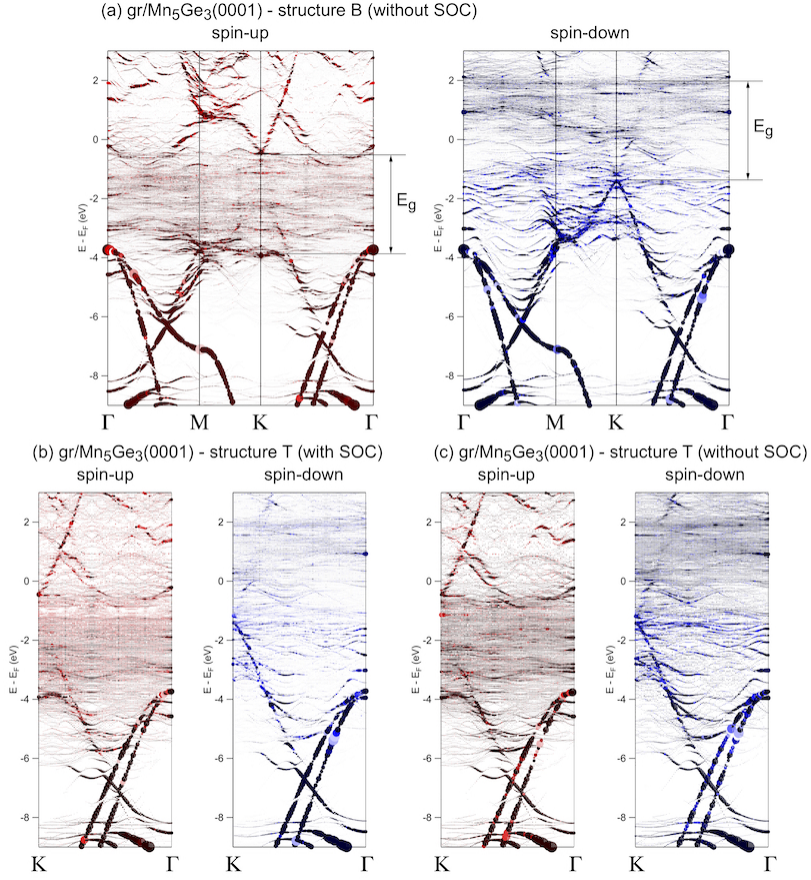


Fig. S6: Large-energy scale spin-resolved band structures for the gr/Mn₅Ge₃(0001) system shown for structure B without (a) and with (b) inclusion of the spin-orbit interaction. In (c) the large-energy scale spin-resolved band structure (without inclusion of the spin-orbit interaction) for structure T is shown. Data in (b) and (c) are shown only for $\Gamma - K$ direction. In (a), the discussed in the main text band gaps for the graphene π states are marked with E_g for spin-up and spin-down channels.